

Near-field-assisted capacity of spoof-plasmonic channels

Mikhail Erementchouk* and Pinaki Mazumder†

*Department of Electrical Engineering and Computer Science,
University of Michigan, Ann Arbor, MI 48109 USA*

Establishing universal features of spoof-plasmonic systems beyond spectral properties is challenging due to the complexity of the specific physical realizations of spoof-plasmonic channels. We introduce a simple 1D scalar model reproducing the key properties of spoof-plasmonic channels and investigate manifestations of plasmonic-like features when only a few local resonances are present. We show that the channel between the source applied to the interior of the structure and the terminal ends (output ports) effectively comprises two subchannels. The activation of one of the subchannels depends on the spatial variation of the source, and therefore, the contribution of this subchannel in conventional systems is small if the source occupies a subwavelength region. We show that, in spoof-plasmonic structures, the activation of this subchannel can enhance significantly in the frequency region where the spoof-plasmonic effects are prominent. This demonstrates that even a few local scattering resonances may strongly impact the flow of wave-carried information.

I. INTRODUCTION

A similarity between the properties of plasmon polaritons and the states of the electromagnetic field near corrugated conducting surfaces has led to the emergence of spoof-plasmonics^{1–3}. Propagation of waves in spoof-plasmonic structures mimics plasmon polaritons opening ways for achieving plasmonic effects across broad frequency intervals, including those that are far below the plasmon frequencies of conventional materials. The physical origin of the emergence of plasmonic features are the resonances at open cavities formed by the corrugations. Since the physical origin of such resonances is secondary, spoof-plasmonics, while established originally for electrodynamic structures^{4,5}, emerges as a manifestations of fundamental properties of wave systems with local resonances. It is, therefore, not surprising that the spoof-plasmonic approach found applications in other wave systems besides electromagnetic, predominately acoustic^{6–12}. Moreover, the physical origin of the local resonances may be different from the nature of propagating waves as was explored in acoustic waveguides in Ref. 11 and in cascade quantum lasers in Ref. 13, where the resonances are formed by excitons in multiple quantum wells^{14,15}.

At the same time, revealing universal features of spoof-plasmonic channels is hindered by the difficulties associated with the first-principle representation of particular physical implementations. The common approach to deal with these difficulties is to employ a version of the effective medium approximation in conjunction with full-wave simulation. One of the drawbacks of the effective medium approach is hiding the effect of local resonances. This excludes the effect of the strong subwavelength scale spatial modulations of the field in the channel, which may play the crucial role in particular applications^{16–18}, and creates an impression that the emergence of spoof-plasmonic effects require many local resonances, similarly to developing photonic crystal effects in modulated dielectric structures.

To address these difficulties and to investigate the emergence of the spoof-plasmonic effects, we introduce a simple 1D scalar model of a spoof-plasmonic channel. The model reveals that such channels demonstrate a plethora of effects associated with the sensitivity of spoof plasmons to subwavelength features at frequencies near the edge of the fundamental spoof plasmonic band. Importantly, the emergence of these effects do not require the presence of many local resonances. In the present paper, we focus to the effect of enhancement of a the signal induced by a source with the spatial variation at the subwavelength scale.

The rest of the paper is organized as follows. In Section II, we introduce the model and solve the main problems regarding the transport properties and the system response. In Section III, we apply these results to demonstrate the enhanced sensitivity with respect to subwavelength variations of the external excitation.

II. SCALAR MODEL WITH DISTRIBUTED LOCAL RESONANCES

As the 1D scalar model of spoof-plasmonic channels we consider a string with attached harmonic oscillators. Denoting the deviations of the string by $\psi(x)$ and of the n -th harmonic oscillator by $\phi^{(n)}(t)$, the equations of motion governing the spatial distribution of deviations from equilibrium in the steady state regime, $\psi(x, t), \phi^{(n)}(t) \propto \exp(-i\omega t)$, can be written as

$$\begin{aligned} k^2 \psi &= -\psi'' + \eta \sum_n \delta(x - x^{(n)}) [\psi(x) - \phi^{(n)}], \\ \omega^2 \phi^{(n)} &= -\Omega_c^2 [\psi(x^{(n)}) - \phi^{(n)}], \end{aligned} \quad (1)$$

where $k = \omega/v$ with v being the speed of waves in the string without oscillators, η is the coupling parameter having the wavenumber dimension, and Ω_c is the natural frequency (with which we associate the respective wavenumber $k_c = \Omega_c/v$) of oscillators attached to an immobilized string.

We adopt the transfer matrix approach, which we briefly overview in Appendix A. The consideration noticeably simplifies if two bases are kept in mind: the Cauchy basis with the state vector $\Psi^{(C)}(x)$ [defined in Eq. (A1)], and the basis based on linearly independent solutions $\Psi^{(w)}(x)$ [Eq. (A3)]. We adopt the notations with the upper index indicating the chosen basis, when the result depends on the explicit form of the transfer matrix and the state vector, and the omitted upper index denoting the basis-independent form.

The transfer matrices are found as the product of transfer matrices across the intervals between the resonances and the transfer matrices across the resonances. According to Eq. (A8), for $x^{(n-1)} < x_1, x_2, < x^{(n)}$, the transfer matrix is

$$\mathcal{T}^{(C)}(x_2, x_1) = \widehat{W}_w(x_2) \widehat{W}_w(x_1)^{-1}, \quad (2)$$

where we have taken into account the transfer matrix in basis of linearly independent solutions is identity, and $\widehat{W}_w(x)$ is the Wronsky matrix given by Eq. (A6).

The transfer matrix across the resonance is the easiest to derive in the Cauchy basis. Enforcing the continuity of the string's displacement at $x = x^{(n)}$, and expressing $\Psi^{(C)}(x^{(n)} + 0)$ in terms of $\Psi^{(C)}(x^{(n)} - 0)$, we find the transfer matrix through the n -th resonance

$$\mathcal{T}^{(C)}(x^{(n)}) = \mathcal{I} + \gamma(\omega) \begin{pmatrix} 0 & 0 \\ 1 & 0 \end{pmatrix}, \quad (3)$$

where $\mathcal{I} = \widehat{1}_2$, a 2×2 identity matrix, $\gamma(\omega) = \eta\omega^2/(\omega^2 - \Omega_c^2)$. The form of the transfer matrix in the basis of independent solutions is obtained using (A8):

$$\mathcal{T}^{(w)}(x^{(n)}) = \mathcal{I} + \frac{i\gamma(\omega)}{2k} \begin{pmatrix} -1 & -e^{-2ikx^{(n)}} \\ e^{2ikx^{(n)}} & 1 \end{pmatrix}. \quad (4)$$

We take a note of a useful basis-independent property $\mathcal{T}(x^{(n)})^N = \mathcal{T}(x^{(n)})|_{\eta \rightarrow N\eta}$.

A. Dispersion relation

Most straightforwardly, the spoof-plasmonic features of the introduced model are demonstrated by the dispersion relation governing the excitations. To this end, we consider a periodic system with period d obtained by replicating the elementary cell occupying the interval $[x_0, x_0 + d]$ with the resonance located at $x^{(0)}$ strictly inside the interval. Consequently, the transfer matrix across the period is

$$\mathcal{T}_P^{(C)} = \mathcal{T}^{(C)}(x_0 + d, x^{(0)}) \mathcal{T}^{(C)}(x^{(0)}) \mathcal{T}^{(C)}(x^{(0)}, x_0). \quad (5)$$

By virtue of the Bloch theorem, the eigenstates of the system must satisfy $\mathcal{T}_P^{(C)} \Psi^{(C)}(x) = e^{i\beta d} \Psi^{(C)}(x)$, where β is the Bloch wavenumber. The relation between ω and

β is found as $\det(\mathcal{T}_P^{(C)} - p) = 0$, where $p = e^{i\beta d}$, which yields the equation $p^2 - p \text{Tr}(\mathcal{T}_P^{(C)}) + \det(\mathcal{T}_P^{(C)}) = 0$. Taking into account that $\det(\mathcal{T}_P^{(C)}) = 1$, we obtain

$$\cos(\beta d) = \frac{1}{2} \text{Tr}(\mathcal{T}_P^{(C)}) = B(\omega; d), \quad (6)$$

where

$$B(\omega; d) = \cos(kd) + \frac{\gamma(\omega)}{2k} \sin(kd). \quad (7)$$

It is edifying to consider an alternative derivation of the dispersion equation mimicking that employed while considering electrodynamic structures^{3,19,20}. This approach relies on constructing the solution to the governing equations of motion based on the Bloch theorem prescribing $\psi(x) = e^{i\beta x} u(x)$, where $u(x)$ is a periodic function with period d . Representing $u(x)$ as a Fourier series, we obtain

$$\psi(x) = \sum_m e^{i\beta_m x} \psi_m, \quad (8)$$

where $\beta_m = \beta + 2\pi m/d$ and ψ_m is the amplitude of the m -th Bloch component. Using this representation in Eq. (1), we find

$$(k^2 - \beta_m^2) \psi_m = \frac{\gamma(\omega)}{d} \sum_{m'} e^{i2\pi(m' - m)x^{(n)}/d} \psi_{m'}. \quad (9)$$

This yields the dispersion equation in the form

$$1 = \frac{\gamma(\omega)}{d} \sum_m \frac{1}{k^2 - \beta_m^2}. \quad (10)$$

While seemingly different, this dispersion equation is equivalent to the one obtained within the transfer matrix approach [Eq. (6)], as we show in Appendix B.

The dispersion equation written in form (10) has the typical structure of dispersion equations describing the spoof plasmonic channels^{5,19,20}. It is not, therefore, surprising that the main features of the dispersion relation governing the excitations of the system under consideration reproduce those of other spoof-plasmonic systems. It is instructive to start with the single mode approximation of Eq.(10) (the approximation often used in studying SSPP). It corresponds to keeping only the term $m = 0$ in the series representation of the dispersion equation, which yields

$$\omega^2(\beta) = \Omega_c^2 - (\Omega_c^2 + \eta v^2/d)^2 \frac{1}{2\beta^2 v^2}. \quad (11)$$

This dispersion relation is similar to the surface plasmon polariton dispersion law with the plasma frequency $\omega_p = \sqrt{2}\Omega_c$. This reveals the main feature of the spoof plasmonic channels emerging at frequencies close to the edge of the fundamental band: the ability to support

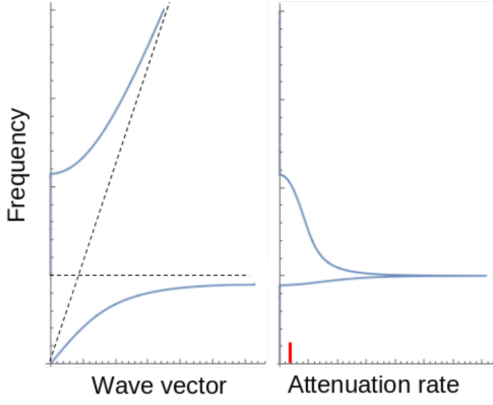


FIG. 1. (Left panel) The overall view of the dispersion diagram inside the first Brillouin zone. (Right panel) The attenuation along the structure inside the spoof-plasmonic gap. The short red line shows the maximum attenuation inside the gap at the boundary of the Brillouin zone (“the photonic crystal” effect). Because of the chosen short period, the frequency corresponding to the anticrossing at the boundary of the Brillouin zone is the order of magnitude higher than the resonance frequency and, therefore, is not shown.

subwavelength features, with the smallest characteristic spatial scale determined by the period of the structure.

At the same time, Eq. (11) demonstrates the typical drawback of the single-mode approximation — the incorrect prediction for the edge of the fundamental band coinciding with the resonance frequency^{20,21}. To obtain the correct value, one needs to consider the exact dispersion equation. In the short-period case, when at the boundary of the Brillouin zone, take $\cos(kd) \approx 1$, $\sin(kd) \approx kd$, we find that the boundary of the fundamental edge is shifted down from Ω_c , so that the resonance frequency is inside the fundamental gap

$$\omega_B^2 = \frac{\Omega_c^2}{1 + \eta d/2}. \quad (12)$$

Using the same approximation, it is straightforward to obtain the dispersion curve for the whole fundamental spoof-plasmonic band:

$$\omega^2(\beta) = \frac{\Omega_c^2}{\sin^2(\beta d/2) + \eta d/2}. \quad (13)$$

The condition determining the upper edge of the first gap, separating the fundamental band from the higher bands, is more complex. However, if it is far below the frequency of the free oscillations at the boundary of the Brillouin zone, $v\beta_B$, one can employ the short period approximation with the slight modification, $\cos(kd) \approx 1 - (kd)^2/2$, and find that the first gap terminates at $\omega_g^2 = \Omega_c^2 + \eta v^2/d$.

The overall shape of the dispersion curves for the first spoof-plasmonic bands is shown in Fig. 1. The curious consequence of the resonance frequency being inside the

gap is that Ω_c splits the gap into two parts with noticeably different properties as is evident from the spectrum of the longitudinal attenuation length (the right panel of Fig. 1). The same effect takes place in electrodynamic SSPP as was found in¹⁶ in conjunction with the resonance tunneling effect and the dependence of the transparency window on the geometry of the defect cell.

B. The effect of decay

In the present paper, we focus on the properties of an ideal system without decay. However, in the realistic systems, the effect of decay should be taken into consideration as it may significantly impact the manifestation of spoof-plasmonic features.

To simplify the analysis, we assume that the main source of decay is the dynamics of resonances, so that the second equation in Eqs. (1) has the form

$$(\omega^2 - \Omega_c^2 + i\alpha_d\omega) \phi^{(n)} = -\Omega_c^2 \psi(x^{(n)}). \quad (14)$$

Following the derivation of the transfer matrix above, it is easy to see that the effect of decay reduces to modifying the expression for $\gamma(\omega)$ defining the transfer matrix through the resonance:

$$\gamma(\omega) = \eta\omega \frac{\omega + i\alpha_d}{\omega^2 - \Omega_c^2 + i\alpha_d\omega}. \quad (15)$$

The decay leads to attenuation of spoof-plasmonic excitations along the structure. Assuming weak decay, we find the attenuation length at the frequency corresponding to the edge of the fundamental band

$$l'' \approx \frac{d^2 \Omega_c \eta}{2\alpha_d}. \quad (16)$$

Notably, the obtained attenuation length depends on the square of the structure period, $l'' \propto d^2$, similarly to its behavior in electrodynamic spoof-plasmonic structures²².

C. Transmission spectra

Overall transport properties of a finite structures inside the interval $[X_A, X_B]$ are described by the reflection and transmission spectra obtained by solving the equations of motion assuming the scattering boundary conditions. In terms of transfer matrices, the solution has the form $\Psi(X_B) = \mathcal{T}(X_B, X_A) \Psi(X_A)$. In turn, the states at the terminating points are written in the basis of independent solutions as $\Psi^{(w)}(X_A) = \mathbf{w}_+ + r_{BA} \mathbf{w}_-$ and $\Psi^{(w)}(X_B) = t_{BA} \mathbf{w}_+$, where $\mathbf{w}_+ = (1, 0)^T$ and $\mathbf{w}_- = (0, 1)^T$, and r_{BA} and t_{BA} are the reflection and transmission coefficients, respectively:

$$\begin{aligned} t_{AB} &= \frac{\det \mathcal{T}(X_B, X_A)}{(\mathbf{w}_-, \mathcal{T}(X_B, X_A) \mathbf{w}_-)}, \\ r_{AB} &= -\frac{(\mathbf{w}_-, \mathcal{T}(X_B, X_A) \mathbf{w}_+)}{(\mathbf{w}_-, \mathcal{T}(X_B, X_A) \mathbf{w}_-)}. \end{aligned} \quad (17)$$

Here, we have defined the inner product as $(\mathbf{a}, \mathbf{b}) := \sum_j a_j^* b_j$ and kept $\det \mathcal{T}(X_B, X_A) = 1$.

D. External excitations

The external source can be incorporated into the system dynamics by adding terms $-F(x)$ and $-F_n$ to the right-hand-side of the first and the second equations of Eqs. (1), respectively. We consider the effect of external sources under “physical” boundary conditions assuming that local resonances and sources are strictly inside of the interval $[X_A, X_B]$, while at the boundary of the interval the excitations satisfy certain boundary conditions. In the present work, we limit our attention only to outgoing boundary conditions so that $\Psi^{(w)}(X_A) \propto \mathbf{w}_-$ and $\Psi^{(w)}(X_B) \propto \mathbf{w}_+$.

The general solution of the equations of motion with the source at points outside of the resonances can be written in the basis-independent form as

$$\Psi(x_2) = \mathcal{T}(x_2, x_1) \Psi(x_1) + \int_{x_1}^{x_2} ds \mathcal{T}(x_2, s) F(s) \mathbf{V}(s), \quad (18)$$

where $\mathbf{V}(s)$ is the vector accounting for the source within the transfer matrix formalism. In the Cauchy basis and the basis of independent solutions, the source vector is

$$\begin{aligned} \mathbf{V}^{(C)}(s) &= \begin{pmatrix} 0 \\ 1 \end{pmatrix}, \\ \mathbf{V}^{(w)}(s) &= \frac{1}{2ik} \begin{pmatrix} e^{-iks} \\ -e^{iks} \end{pmatrix}. \end{aligned} \quad (19)$$

We will assume for simplicity that the source is applied outside of resonances ($F_n \equiv 0$). It should be noted that this assumption does not lose generality, if under the integral in Eq. (18) for $x_2 > x_1$, one adopts the convention $\hat{T}(x_2, s) = \hat{T}(x_2, s + 0)$ and correctly defines the respective $F(s)$. Namely, let the n -th resonance be excited with the source of amplitude F_n . Then, its contribution to $\Psi^{(C)}(x_2)$ in (18) written in the Cauchy basis has the form

$$\gamma(\omega) F_n \hat{T}^{(C)}(x_2, x^{(n)} + 0) \mathbf{V}^{(C)}(s), \quad (20)$$

where transfer matrix $\hat{T}^{(C)}(x_2, x^{(n)} + 0)$ does not include the transfer matrix across the n -th resonance itself.

In what follows we will be specifically interested in the situation when the field is detected at the terminal points (output ports) of the structure. For such situations, the effect of the external excitation can be expressed by a single source vector. It is straightforward to check that choosing a point \bar{X} inside the structure, $X_A < \bar{X} < X_B$, one has

$$\Psi(X_B) = \mathcal{T}(X_B, X_A) \Psi(X_A) + \mathcal{T}(X_B, \bar{X}) \bar{\mathbf{V}}(\bar{X}), \quad (21)$$

where we introduced a representing source vector

$$\bar{\mathbf{V}}(\bar{X}) = \int_{X_A}^{X_B} ds \mathcal{T}(\bar{X}, s) F(s) \mathbf{V}(s). \quad (22)$$

To illustrate the difference between the free (without the local resonances) and spoof-plasmonic systems, we consider the effect of canceled output of two point sources separated by a subwavelength distance. The outgoing boundary conditions ensure that this effect takes place when $\bar{\mathbf{V}} = 0$. Let the sources be applied at points $s_1 = -d_1$ and $s_2 = d_2$, with positive d_1 and d_2 , so that $F(s) = f_1 \delta(s - s_1) + f_2 \delta(s - s_2)$. Then, writing Eq. (22) in the basis of independent solutions, we obtain for the free system

$$\bar{\mathbf{V}}_{\text{free}} = f_1 \mathbf{V}(s_1) + f_2 \mathbf{V}(s_2). \quad (23)$$

The condition of existence of nontrivial solutions to $\bar{\mathbf{V}}_{\text{free}} = 0$ is the easiest to obtain by writing the source representing vector in the basis of independent solutions: $\sin(k(d_1 + d_2)) = 0$. Thus, for close sources, with $k(d_1 + d_2) < \pi$, this condition cannot be met.

The presence of local resonances in the spoof-plasmonic channel changes the situation drastically. It should be noted that if the source locations are not separated by a local resonance, one can choose $\bar{X} > s_2$ in such a way that the interval $[s_1, \bar{X}]$ does not contain local resonances. In this case, the source representing vector is determined by the same Eq. (23) as for the free system, leading to the no-cancellation outcome.

Let the sources be placed in the same way as for the free system with the local resonance between them, $x^{(0)} = 0$. Then, we have

$$\bar{\mathbf{V}}_{\text{SP}} = f_1 \mathcal{T}_0 \mathbf{V}(s_1) + f_2 \mathbf{V}(s_2), \quad (24)$$

where we have introduced $\mathcal{T}_0 = \mathcal{T}(x^{(0)})$.

The condition for the existence of a non-trivial solution to $\bar{\mathbf{V}}_{\text{SP}}^{(w)} = 0$ is found to be

$$\sin(k(d_1 + d_2)) + \frac{\gamma(\omega)}{2k} \sin(kd_1) \sin(kd_2) = 0, \quad (25)$$

which can be satisfied even for subwavelength separation of the sources.

We consider in more detail the case of symmetric placement of sources around the resonance: $d_1 = d_2 = d$. In this case, the cancellation condition has the form $B(\omega; d) = 0$ and corresponds to the edge of the spoof-plasmon fundamental band in the structure with period d . When the condition is met, the nontrivial solution to Eq. (24) is $f_1 = f_2 \neq 0$. Figure 2 compares the response of the system when the cancellation condition is met and the system is tuned away from the cancellation frequency.

It is worth emphasizing that the cancellation occurs at the edge of the fundamental spoof-plasmonic band [Eq. (12)]. This is an example of the emergence of spoof-plasmonic features that are commonly associated with periodic systems in short systems containing only few local resonances¹⁶.

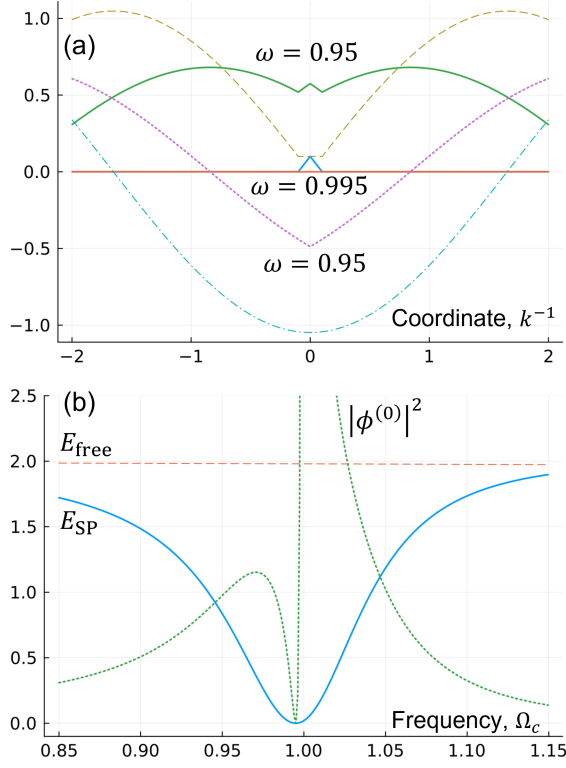


FIG. 2. The two-source cancellation in spoof-plasmonic channels. (a) The response of the free system (dashed and dashed dotted lines show, $\text{Re}[\psi(x)]$, and $\text{Im}[\psi(x)]$, respectively) at $\omega/\Omega_c = 0.95$, and spoof-plasmonic systems at $\omega/\Omega_c = 0.95$ (the cancellation condition is not met) and $\omega/\Omega_c = 0.995$ (the condition is met). Solid and dotted lines show $\text{Re}[\psi(x)]$ and $\text{Im}[\psi(x)]$, respectively. (b) The frequency dependence of the outgoing signal $E_j(\omega) = |\psi(X_A)|^2 + |\psi(X_B)|^2$ with $j = \text{free}$ (dashed line) and $j = \text{SP}$ (solid line) for the free and spoof-plasmonic systems, respectively. The dotted line shows the magnitude of the local resonance excitation $|\phi^{(0)}(\omega)|^2$.

III. NEAR-FIELD-ASSISTED INFORMATION CHANNEL CAPACITY

A source applied inside the structure creates a signal at both terminating points of the structure implying the information flow from the source to the output ports. An important feature of spoof-plasmonics systems is revealed when one considers the source distributed over a region of a subwavelength size. In this case, the information flow can be regarded as carried by two simple channels activated by the long-scale and the short-scale features of the source distribution. In the free system, the short-scale channel remains only weakly activated owing to the small size of the excitation region. However, in the spoof-plasmonic systems, in the frequency region where the plasmonic features become prominent, the contribution of the short-scale channel can significantly increase.

The capacity of the channel between the source S and

the output ports AB is defined as $\max_{P_S} I(AB : S)$, where $I(AB : S)$ is the mutual information of the source and the output ports, and the maximum is taken over the distribution functions describing the source, P_S . This definition can be simplified by taking into account that, by virtue of the outgoing boundary conditions, the output state is given in the basis of independent solutions by $\Psi^{(w)}(X_A) = c_- \mathbf{w}_-$ and $\Psi^{(w)}(X_B) = c_+ \mathbf{w}_+$. It is convenient to represent the state in a vector form $\mathbf{c} = (c_+, c_-)^T \in \mathbb{C}^2$. Consequently, the same situation as above, with two point sources, is sufficient to consider the channel capacity without loss of generality as long as vectors $\mathbf{V}^{(w)}(s_1)$ and $\mathbf{V}^{(w)}(s_2)$ are linearly independent. Introducing the vector notation for the source amplitudes $\mathbf{f} = (f_1, f_2)^T \in \mathbb{C}^2$, we have a relation between the output signal and the source $\mathbf{c} = \hat{G}\mathbf{f}$. The matrix elements of \hat{G} (the transfer function) are found using Eqs. (21) and (22)

$$\begin{aligned} G_{1j} &= t_{AB} \left(\mathbf{w}_+, \mathcal{T}(X_A, s_j) \mathbf{V}^{(w)}(s_j) \right), \\ G_{2j} &= -t_{AB} \left(\mathbf{w}_-, \mathcal{T}(X_B, s_j) \mathbf{V}^{(w)}(s_j) \right), \end{aligned} \quad (26)$$

where $j = 1, 2$. While deriving (26), we have taken into account that $\mathcal{T}(X_A, X_B) = \mathcal{T}^{-1}(X_B, X_A)$ and the relation between the matrix elements of 2×2 matrices: $T_{22} = (T^{-1})_{11}$.

Such obtained relation between the output and the sources allows one to use the standard approach for multivariate Gaussian channels and write down the channel capacity as (see, e.g. Ref 23 and 24)

$$C_{\text{SP}} = \max_{\hat{K}_f} \frac{1}{2} \log \left[\det \left(1 + \frac{S}{\nu} \hat{G} \hat{K}_f \hat{G}^\dagger \right) \right], \quad (27)$$

where S/ν is the signal-to-noise ratio, $\hat{K}_f = \langle \mathbf{f} \times \mathbf{f}^\dagger \rangle$ is the (normalized) source covariance matrix, and the maximum is taken over all admissible covariance matrices.

Individual subchannels contributing to C_{SP} in (27) can be identified as the basis, in which transfer function \hat{G} is diagonal, so that $g^{(j)}$, the eigenvalues of \hat{G} , have the meaning of the subchannel scalar transfer functions. For example, assuming that the input does not mix the channels, Eq. (27) turns into $C_{\text{SP}} = \sum_j C_{\text{SP}}^{(j)}$, where j runs over the channels, and $C_{\text{SP}}^{(j)}$ is the capacity of the j -th subchannel:

$$C_{\text{SP}}^{(j)} = \frac{1}{2} \log \left(1 + \frac{\langle |f^{(j)}|^2 \rangle}{\nu} |g^{(j)}|^2 \right). \quad (28)$$

With this perspective in mind and to avoid the application-specific questions regarding the choice of the source covariance matrix, we limit our consideration to the transfer functions of individual channels. To make apparent the emergence of channels associated with different scales of the source spatial variation, we consider

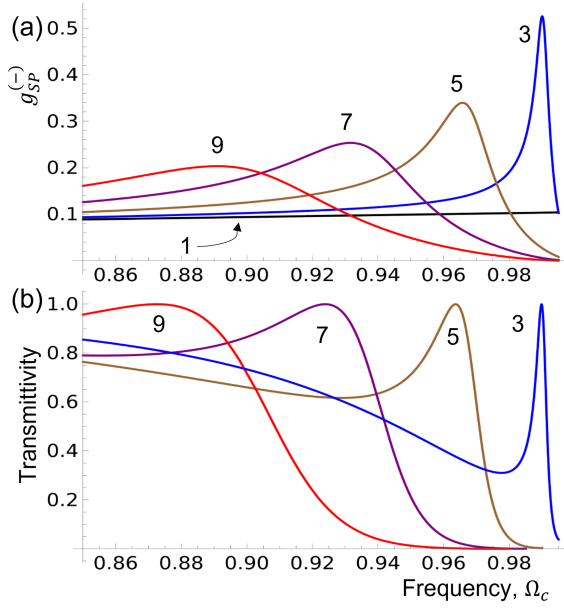


FIG. 3. (a) The frequency dependence of the scalar transfer function $g_{\text{SP}}^{(-)}(\omega)$ carrying the signal induced by the details of the source spatial variation for structures with $2N + 1 = 3, 5, 7, 9$ local resonances. The separation between the sources and the local resonances is chosen $0.1/k_c$. The line corresponding to only one local resonance coincides with the transfer function of the free system. (b) The transmission spectrum, $|t_{AB}(\omega)|^2$, for the same structures.

the case, when the systems and the source placement has the inversion symmetry. In other words, we consider sources placed at $s_{1,2} = \pm d$ in a system with local resonances at $x^{(n)} = pn$ with $p > d$ and $-N \leq n \leq N$.

In this case, the transfer function \hat{G} preserves the symmetry (symmetric and antisymmetric distributions) of the source and is diagonalized by $\hat{M} = \begin{pmatrix} 1 & 1 \\ 1 & -1 \end{pmatrix} / \sqrt{2}$

$$\tilde{G} = \hat{M} \hat{G} \hat{M}^{-1} = \begin{pmatrix} g^{(+)} & 0 \\ 0 & g^{(-)} \end{pmatrix}, \quad (29)$$

where the eigenvalues $g^{(\pm)}$ have the meaning of the scalar transfer functions corresponding to the channels activated by the symmetric and antisymmetric sources. From the perspective of the source spatial distribution, $g^{(+)}$ transfers the signal corresponding to the spatially averaged source, while $g^{(-)}$ carries the signal determined by the short-scale features of the source distribution.

This distinction becomes apparent for the free system, for which one has $g^{(\pm)} = (\mathbf{w}_{\pm}, \mathbf{V}^{(w)}(s_1) \pm \mathbf{V}^{(w)}(s_2))$, so that $g_{\text{free}}^{(+)}(d) = \cos(kd)/ik$ and $g_{\text{free}}^{(-)}(d) = \sin(kd)/k$. For sources confined to a subwavelength interval, one has $g_{\text{free}}^{(-)}(d) \ll 1$, and the short-scale channel remains under-activated.

In the spoof-plasmonic system, the capacity of the short-scale channel is modified, compared to the free system, by the resonances. Introducing $\mathcal{T}(X_B, x^{(0)}) \equiv$

$\mathcal{T}(X_B, x^{(0)} + 0) \mathcal{T}_0^{1/2}$, we obtain our main result

$$g_{\text{SP}}^{(-)} = g_{\text{free}}^{(-)}(d) t_{AB} \left(\mathbf{w}_{-}, \mathcal{T}^{(w)} \left(X_B, x^{(0)} \right) \begin{pmatrix} 1 \\ 1 \end{pmatrix} \right). \quad (30)$$

It is constructive to consider the case when the structure, similarly to the consideration of the cancellation effect, contains only one local resonance. In this case, one has $t_{AB} = (1 + i\gamma/2k)^{-1}$, and, as a result, the transfer function coincides with that for the free system. This is utilized in Fig. 3 illustrating that the overall frequency dependence of $g_{\text{SP}}^{(-)}$ is mainly determined by the transmission spectrum of the structure.

To show the enhancement more explicitly, we use the fact that the local resonance at $x^{(0)}$ does not affect the contribution of the antisymmetric component and consider the simplest structure where the enhancement takes place: with resonances at $x^{(\pm 1)} = \pm p$ and sources at $s_{1,2} = \mp d$. For this case, we obtain

$$g_{\text{SP}}^{(-)}(d) = g_{\text{free}}^{(-)}(d) \frac{e^{-ikp}}{B_2(\omega; p) + i \sin(kp)}, \quad (31)$$

where $B_2(\omega; p) = \cos(kp) + (\gamma/k) \sin(kp)$ has the meaning of the dispersion equation of spoof plasmons with the modified coupling constant $\eta \rightarrow 2\eta$. Equation (31) shows that $g_{\text{free}}^{(-)}$ is modified by a resonance centered at the edge of the fundamental band of the modified and with the width $2k_c \sin^2(k_c p) / \eta \cos(k_c p)$. We find that the maximal value of the enhancement factor is $|g_{\text{SP}}^{(-)} / g_{\text{free}}^{(-)}| = 1 / \sin(k_c p)$. For example, using $p = 0.1k_c^{-1}$, as in Fig. 3, we obtain about five-fold enhancement.

The dependence of the transfer function of the long-scale channel, $g_{\text{SP}}^{(+)}$, on the separation of the sources reflects the cancellation effect discussed above

$$g_{\text{SP}}^{(+)} = \frac{B(\omega; d)}{ik} t_{AB} \left(\mathbf{w}_{-}, \mathcal{T}^{(w)} \left(X_B, x^{(0)} \right) \begin{pmatrix} 1 \\ -1 \end{pmatrix} \right). \quad (32)$$

A curious feature of $g_{\text{SP}}^{(+)}(\omega)$ is the emergence of narrow resonances near the edge of the fundamental spoof-plasmonic band. Similarly to $g_{\text{SP}}^{(-)}(\omega)$, these resonances are caused by transmission resonances, as illustrated by Fig. 4. It must be noted, however, that due to the proximity of these resonances to the edge of the fundamental band, they can be expected to be strongly affected by the decay. As a result, the significance of these resonances in particular physical implementations of spoof-plasmonic channels may be significantly reduced and should be studied on the case-by-case basis.

We conclude by noticing that the inversion symmetry simplifies finding the explicit form of the spoof plasmonic modes of the structure. The role of the symmetrical placement of the sources is secondary as any source can be decomposed as a superposition of contributions with definite symmetry (projections on the respective irreducible representations). Indeed, using the

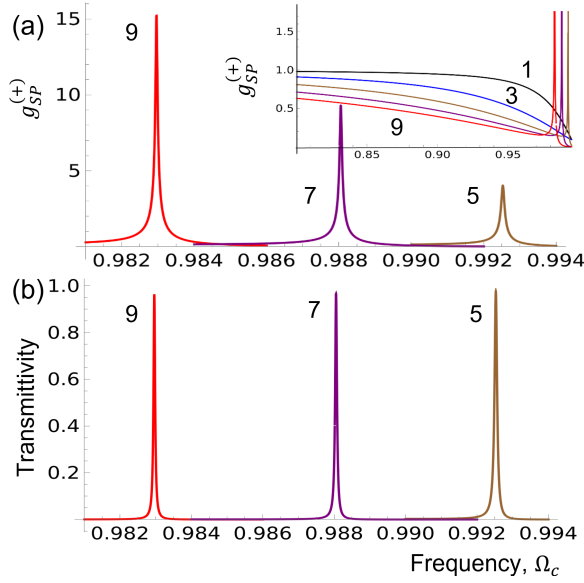


FIG. 4. (a) The fine details of the frequency dependence of the scalar transfer function $g_{SP}^{(+)}(\omega)$ near the resonances for structures with $2N + 1 = 5, 7, 9$ local resonances. The inset shows $g_{SP}^{(+)}(\omega)$ in a wide frequency interval. (b) The transmission resonances, $|t_{AB}(\omega)|^2$, responsible for resonances in the transfer function.

notion of the transfer matrix from the center of the structure, $\mathcal{T}(X_B, x^{(0)})$, we can choose $\bar{X} = x^{(0)}$ and define the source representing vector at the center of the structure $\bar{\mathbf{V}}_0 = \bar{\mathbf{V}}(x^{(0)})$, with

$$\bar{\mathbf{V}}^{(w)}(x^{(0)}) = f_1 \mathcal{T}_0^{1/2} \mathbf{V}(s_1) + f_2 \mathcal{T}_0^{-1/2} \mathbf{V}(s_2), \quad (33)$$

so that the last term in Eq. (21) has the form $\mathcal{T}(X_B, x^{(0)}) \bar{\mathbf{V}}_0$. Thus, we obtain for $s_1 = x^{(0)} - d_1$ and $s_2 = x^{(0)} + d_2$

$$\begin{aligned} \bar{\mathbf{V}}_0^{(w)} &= \frac{1}{2ik} [f_1 B(\omega; d_1) + f_2 B(\omega; d_2)] \begin{pmatrix} 1 \\ -1 \end{pmatrix} \\ &\quad \frac{1}{2k} [f_1 \sin(kd_1) - f_2 \sin(kd_2)] \begin{pmatrix} 1 \\ 1 \end{pmatrix}. \end{aligned} \quad (34)$$

Here, the first and the second terms in the right-hand side represent symmetric and antisymmetric components, respectively. Representation (34) explicitly expresses the fact that the local resonance placed between the sources does not affect the antisymmetric component, as has been used above for evaluating the enhancement factor.

IV. CONCLUSION

We considered a simplified 1D scalar model of spoof-plasmonic channels. Mechanically, the model can be represented as a string with attached harmonic oscillators playing the role of local leaky resonances. We show

that the model reproduces main spectral feature of spoof-plasmonic channels, including such subtle effects as a the red-shift of the fundamental band from the resonance frequency and the dependence of the attenuation length on the square of the structure period.

Owing to its simplicity, the model allows investigating features that are to challenging to establish within the frameworks of first-principle descriptions. We use this opportunity to investigate manifestations of plasmonic-like features in structures with only few local resonances.

The main result is the enhanced sensitivity of the signal induced in the structure by the source on the spatial variation of the source at the subwavelength scale. The sensitivity is characterized from the perspective of the informational capacity of the channel between the source and the output ports (terminating ends of the structure). It is shown that while this channel comprises two subchannels, the activation of one of subchannels depends on the size of the region where the source is applied. As a result, if the source region is of the subwavelength size, the subchannel is characterized by a small channel capacity in conventional systems. However, spoof-plasmonic structures demonstrate enhancement of the short-scale subchannel in the frequency region where the spoof-plasmonic effects are prominent.

From a more general perspective, this effect demonstrates that the flow of information carried by waves can be significantly impacted by strong scattering resonances even if only a few of such resonances are present.

ACKNOWLEDGMENT

The work has been supported by the US National Science Foundation (NSF) under Grant No. 1909937.

Appendix A: Bases in the transfer matrix formalism

The transfer matrix $\mathcal{T}(x_2, x_1)$ relates state vectors at two points

$$\Psi(x_2) = \mathcal{T}(x_2, x_1) \Psi(x_1). \quad (A1)$$

The main actively employs the fact that the state vector can be specified in different ways to better accommodate the specifics of a particular problem. The explicit form of the transfer matrix depends on the choice of the representation of the local state, which can be regarded as choosing the basis for the state vector. Here, we provide the relation between the transfer matrices given in two bases used in the main text.

The first basis utilizes the observation that a solution of the second order ODE with respect to $\psi(x)$ is specified by providing the pair $\psi(x_1)$ and $\psi'(x_1)$ at some point x_1 . This leads to the state vector

$$\Psi^{(C)}(x) = \begin{pmatrix} \psi(x) \\ \psi'(x) \end{pmatrix}. \quad (A2)$$

Within the remaining parts of the interval, $\psi(x)$, and hence $\Psi(x)$, is found by solving the governing ODE as the Cauchy problem treating $\Psi(x_1)$ as the initial condition: $\Psi^{(C)}(x_2) = \mathcal{T}^{(C)}(x_2, x_1) \Psi^{(C)}(x_1)$. Because of this, we will refer to $\Psi^{(C)}(x)$ and $\mathcal{T}^{(C)}(x_2, x_1)$ as written in the Cauchy basis.

An alternative approach to specifying the state vector uses a pair of linearly independent functions, $h_{1,2}(x)$:

$$\Psi^{(h)}(x) = \begin{pmatrix} c_1(x) \\ c_2(x) \end{pmatrix}, \quad (\text{A3})$$

where the superscript h signifies the functions pair, and the amplitudes $c_{1,2}(x)$ are found as the solution of the system of equations

$$\begin{aligned} \psi(x) &= c_1(x)h_1(x) + c_2(x)h_2(x), \\ \psi'(x) &= c_1(x)h_1'(x) + c_2(x)h_2'(x). \end{aligned} \quad (\text{A4})$$

The existence of solutions is warranted by the linear independence of vectors $(h_1(x), h_1'(x))^T$ and $(h_2(x), h_2'(x))^T$, that is at points where the Wronsky matrix

$$\widehat{W}_h(x) = \begin{pmatrix} h_1(x) & h_2(x) \\ h_1'(x) & h_2'(x) \end{pmatrix}. \quad (\text{A5})$$

is nonsingular.

A particularly convenient choice is the pair of independent solutions of the governing ODE: $h_1 = w_+(x)$, $h_2 = w_-(x)$. For example, for a free wavesystem at the frequency corresponding to wavenumber k , it is convenient to choose $w_{\pm}(x) = e^{\pm ikx}$, in which case the Wronsky matrix takes the form

$$\widehat{W}_w(x) = \begin{pmatrix} e^{ikx} & e^{-ikx} \\ ike^{ikx} & -ike^{-ikx} \end{pmatrix}. \quad (\text{A6})$$

We will say that the state vector is written in the basis of independent solutions. In this basis the transfer matrix is trivial $T^{(w)}(x_2, x_1) = \widehat{1}$.

Equations (A4) provide the relation between state vectors in different bases:

$$\Psi^{(C)}(x) = \widehat{W}_h(x) \Psi^{(h)}(x), \quad (\text{A7})$$

which leads to

$$\mathcal{T}^{(h)}(x_2, x_1) = \widehat{W}_h^{-1}(x_2) \mathcal{T}^{(C)}(x_2, x_1) \widehat{W}_h(x_1). \quad (\text{A8})$$

We note that the relation between transfer matrices in different bases is not a similarity transformation.

Appendix B: Equivalence of different forms of the dispersion equation

To show the equivalence of

$$\cos(\beta d) = \cos(kd) + \frac{\gamma}{2k} \sin(kd). \quad (\text{B1})$$

and

$$1 = \frac{\gamma}{d} \sum_m \frac{1}{k^2 - \beta_m^2}, \quad (\text{B2})$$

with $\beta_m = \beta + 2\pi \frac{m}{d}$, we, first, rewrite Eq. (B2) as

$$\begin{aligned} \frac{2k}{\gamma} &= \frac{1}{\varphi_+} + \frac{1}{\varphi_-} + \\ &\sum_{m>0} \left(\frac{2\varphi_+}{\varphi_+^2 - (2\pi m)^2} + \frac{2\varphi_-}{\varphi_-^2 - (2\pi m)^2} \right), \end{aligned} \quad (\text{B3})$$

where $\varphi_{\pm} = d(k \pm \beta)$. Next, we observe that

$$\frac{2\varphi}{\varphi^2 - (2\pi m)^2} = \frac{\partial}{\partial \varphi} \ln \left(1 - \left(\frac{\varphi}{2\pi m} \right)^2 \right). \quad (\text{B4})$$

Thus, we have for the sum in the r.h.s. of (B3)

$$\begin{aligned} \sum_{m>0} &= \frac{\partial}{\partial \varphi_+} \ln \left[\prod_{m=1}^{\infty} \left(1 - \left(\frac{\varphi_+}{2\pi m} \right)^2 \right) \right] + \\ &\frac{\partial}{\partial \varphi_-} \ln \left[\prod_{m=1}^{\infty} \left(1 - \left(\frac{\varphi_-}{2\pi m} \right)^2 \right) \right] \end{aligned} \quad (\text{B5})$$

Using the Euler infinite product representation,

$$\frac{\sin(\pi z)}{\pi z} = \prod_{m>0} \left(1 - \left(\frac{z}{m} \right)^2 \right), \quad (\text{B6})$$

we obtain

$$\begin{aligned} \frac{2k}{\gamma} &= \frac{1}{\varphi_+} + \frac{1}{\varphi_-} + \\ &\frac{\partial}{\partial \varphi_+} \ln \left[\frac{\sin(\varphi_+/2)}{\varphi_+/2} \right] + \frac{\partial}{\partial \varphi_-} \ln \left[\frac{\sin(\varphi_-/2)}{\varphi_-/2} \right], \end{aligned} \quad (\text{B7})$$

which simplifies to

$$\frac{2k}{\gamma} = \frac{\cos(\varphi_+/2)}{2 \sin(\varphi_+/2)} + \frac{\cos(\varphi_-/2)}{2 \sin(\varphi_-/2)}. \quad (\text{B8})$$

This expression is straightforward to reshape to form (B1).

-
- * merement@gmail.com
† pinakimazum@gmail.com
- ¹ P. A. Huidobro, A. I. Fernández-Domínguez, J. B. Pendry, L. Martín-Moreno, and F. J. García-Vidal, *Spoof Surface Plasmon Metamaterials*, 1st ed. (Cambridge University Press, 2018).
 - ² W. X. Tang, H. C. Zhang, H. F. Ma, W. X. Jiang, and T. J. Cui, *Advanced Optical Materials* **7**, 1800421 (2019).
 - ³ F. J. García-Vidal, A. I. Fernández-Domínguez, L. Martín-Moreno, H. C. Zhang, W. Tang, R. Peng, and T. J. Cui, *Reviews of Modern Physics* **94**, 025004 (2022).
 - ⁴ J. B. Pendry, L. Martín-Moreno, and F. J. García-Vidal, *Science* **305**, 847 (2004).
 - ⁵ F. J. García-Vidal, L. Martín-Moreno, and J. B. Pendry, *Journal of Optics A: Pure and Applied Optics* **7**, S97 (2005).
 - ⁶ J. Christensen, A. I. Fernandez-Dominguez, F. de Leon-Perez, L. Martin-Moreno, and F. J. Garcia-Vidal, *Nature Physics* **3**, 851 (2007).
 - ⁷ J. Christensen, L. Martín-Moreno, and F. J. García-Vidal, *Physical Review B* **81**, 174104 (2010).
 - ⁸ G. Ma and P. Sheng, *Science Advances* **2**, e1501595 (2016).
 - ⁹ N. Cselyuszká, A. Alù, and N. Janković, *Physical Review Applied* **12**, 054014 (2019).
 - ¹⁰ N. Janković, S. Ilić, V. Bengin, S. Birgermajer, V. Radonić, and A. Alù, *Results in Physics* **28**, 104645 (2021).
 - ¹¹ J. jin Park, J.-H. Kwak, and K. Song, *Extreme Mechanics Letters* **43**, 101203 (2021).
 - ¹² K. Pham and A. Maurel, *Physical Review B* **108**, 024303 (2023).
 - ¹³ G. Sun, J. B. Khurgin, and D. P. Tsai, *Optics Express* **21**, 28054 (2013).
 - ¹⁴ L. I. Deych and A. A. Lisyansky, *Physical Review B* **62**, 4242 (2000).
 - ¹⁵ E. L. Ivchenko, *Optical Spectroscopy of Semiconductor Nanostructures* (Alpha Science International Ltd, Harrow, UK, 2005).
 - ¹⁶ S. R. Joy, M. Erementchouk, and P. Mazumder, *Physical Review B* **95**, 075435 (2017).
 - ¹⁷ M. Aghadjani, M. Erementchouk, and P. Mazumder, *Journal of Optical Society of America B* **35**, 1113 (2018).
 - ¹⁸ R. Shugayev, J. Devkota, S. Crawford, P. Lu, and M. Buric, *Advanced Quantum Technologies* **4**, 2000151 (2021).
 - ¹⁹ K. Song and P. Mazumder, *IEEE Transactions on Electron Devices* **56**, 2792 (2009).
 - ²⁰ M. Erementchouk, S. R. Joy, and P. Mazumder, *Proceedings of the Royal Society A: Mathematical, Physical and Engineering Sciences* **472**, 20160616 (2016).
 - ²¹ O. Schnitzer, *Physical Review B* **96**, 085424 (2017).
 - ²² A. Rusina, M. Durach, and M. I. Stockman, *Applied Physics A* **100**, 375 (2010).
 - ²³ G. Foschini and M. Gans, *Wireless Personal Communications* **6**, 311 (1998).
 - ²⁴ E. Telatar, *European Transactions on Telecommunications* **10**, 585 (1999).